J. Fluid Mech. (1975), vol. 72, part 2, pp. 257–268
Printed in Great Britain


# Developing flow in circular conduits: transition from plug flow to tube flow

By M. H. WAGNER
Institut für Kunststofftechnologie (IKT),
University of Stuttgart, Germany

(Received 27 January 1975 and in revised form 14 July 1975)

A numerical solution of the complete Navier–Stokes equations of motion by means of an implicit finite-difference method is presented for the following developing-flow problem: a piston forced with constant speed through an infinitely long tube of circular cross-section. The transition of the velocity profile of an incompressible isothermal Newtonian fluid from the plug-flow profile in front of the piston to the parabolic profile of developed flow is analysed. Streamlines, vorticity distributions, velocity profiles, the excess pressure drop and the entrance length are given for Reynolds numbers from 0 to 800.

## 1. Introduction

The development of plane or axisymmetric steady laminar flow of a liquid flowing into a channel between two semi-infinite parallel plates or into a semi-infinite tube is one of the most widely studied problems of hydrodynamics. This is due to both its technical importance and its ability to demonstrate certain mportant effects of viscous flow.

Since the pioneering work of Prandtl, boundary-layer theory has been the principal tool for solving this developing-flow problem in the high Reynolds number limit, replacing the elliptic Navier–Stokes equations by their parabolic asymptotic forms, the boundary-layer equations. A thorough analysis of this method for plane entry flow has been given by Van Dyke (1970) and Wilson (1971), who resolved a paradox in the classical solution of Schlichting (1934). Reference to experimental data has been provided by Sparrow, Lin & Lundgren (1964) and by Schmidt & Zeldin (1969).

The widespread use of digital computation and sophisticated numerical methods led to the solution of the complete Navier–Stokes equations of motion in the lower Reynolds number regime. The flow at the entrance of a pipe was analysed by numerous investigators both by finite-difference and by finite-element methods. Reference is made here only to the work of Vrentas & Duda (1973), who presented summaries of such entrance-flow studies along with finite-difference solutions of entrance-flow problems for Newtonian and non-Newtonian fluids.

One difficulty associated with this kind of developing-flow problem is the specification of appropriate inlet conditions. This is due to the fact that the developing velocity field in the entrance section of the conduit will significantly influence the velocity field in the upstream region. Various inlet conditions were therefore used in these investigations. For example, Friedmann, Gillis & Liron (1968) assumed an initially uniform velocity profile, whereas Vrentas, Duda & Bargeron (1966) used a streamtube model. In the boundary-layer approximation, Van Dyke (1970) and Wilson (1971) considered three different inlet conditions at the channel entrance, namely uniform velocity, irrotational flow and an infinite cascade of parallel plates (which is equivalent to the streamtube model in axisymmetric flow). As Wilson (1971) pointed out, the least satisfactory model (uniform entry) is the one most commonly studied, in contrast to the most suitable one (infinite cascade).

So far, a different developing-flow problem with clearly defined boundary conditions has received little attention: fluid forced through an infinitely long tube by a piston moving with constant speed. The velocity profile, which is flat at the front of the piston, changes with increasing distance from the piston until a fully developed, parabolic velocity distribution is reached (figure 1*a*). Correspondingly, the pressure gradient in the hydrodynamic entrance region differs from that in the region of fully developed flow. Establishing the detailed nature of this kind of flow is of considerable interest because of its technical importance. The present study was inspired especially by the plastics injection moulding process and capillary rheometry. Typical Reynolds numbers for these applications ($10^{-6}$–10) are close to the creeping-flow limit, but computation was extended to higher Reynolds numbers, up to $Re = 800$.

The only other theoretical work on the subject known to the author is the investigation of Gerrard (1971), who analysed the unsteady axisymmetric pipe flow close to a piston by an explicit finite-difference method. In contrast to the present study, which considers the steady flow problem, Gerrard was concerned with the time dependence of flow started from rest by both impulsive and gradual motion of the piston to Reynolds numbers of 525 and 1000. Experimentally observed ring vortices (Hughes & Gerrard 1971) in the impulsively started flow for Reynolds numbers above approximately 450 were only reproduced by computation after an additional random disturbance had been applied to the flow field at each time step. These ring vortices died out at later times, but no details of steady flow patterns requiring long computation times were given.

Further experimental work on the piston flow problem was reported by Tabaczynski, Hoult & Keck (1970), who studied the transition to turbulence in the ring vortices produced by the starting motion of the piston at even higher Reynolds numbers. The flow close to an oscillating piston in a tube was investigated by Gerrard & Hughes (1971).

In the present study, the steady-state vorticity equation and the continuity equation were solved for the piston flow problem by an implicit finite-difference method for Reynolds numbers from 0 to 800. An implicit method, similar to the one used by Vrentas *et al.* (1966), was chosen instead of an explicit method because of greater numerical stability and less dependence on the mesh size. The computations were performed on a CDC 6600 computer at the Recheninstitut der Universität Stuttgart; run times of up to 5 min were required for a mesh with 3721 grid points.

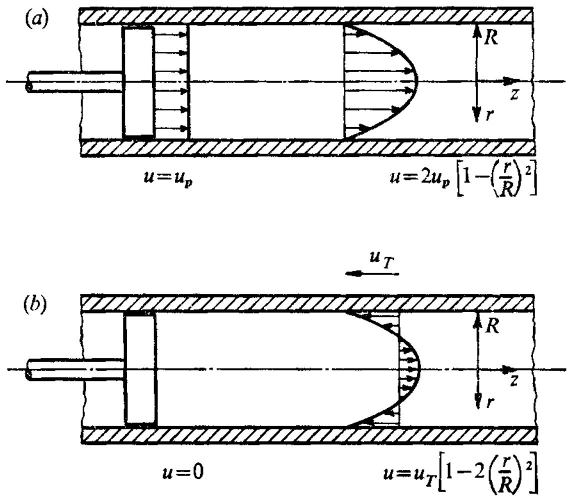


FIGURE 1. Transition from plug flow to tube flow.

## 2. The basic equations

Isothermal steady-state laminar flow of an incompressible Newtonian fluid with constant viscosity is considered. The fluid is forced through an infinitely long tube by a piston moving with constant speed. An identical flow field will be achieved when, instead of keeping the tube fixed in space and the piston moving (figure 1*a*), the piston is fixed in space and the tube is moved in the opposite direction with the same speed (figure 1*b*). The first case will be referred to as the 'tube space' problem, the second, which is more convenient for analysis and will be used subsequently if not stated otherwise, as the 'piston space' problem, according to the frame of reference. The two spaces are connected to each other by a simple co-ordinate transformation.

Restricting the analysis to a circular conduit with no leakage between the tube wall and the piston, and neglecting the body-force term, the dimensionless equations of motion and the continuity equation reduce to

$$v\frac{\partial v}{\partial r}+u\frac{\partial v}{\partial z} = -\frac{\partial p}{\partial r}+\frac{2}{Re}\left(\frac{\partial}{\partial r}\left[\frac{1}{r}\frac{\partial}{\partial r}(rv)\right]+\frac{\partial^2 v}{\partial z^2}\right), \tag{1}$$

$$v\frac{\partial u}{\partial r}+u\frac{\partial u}{\partial z} = -\frac{\partial p}{\partial z}+\frac{2}{Re}\left(\frac{1}{r}\frac{\partial}{\partial r}\left[r\frac{\partial u}{\partial r}\right]+\frac{\partial^2 u}{\partial z^2}\right), \tag{2}$$

$$\frac{1}{r}\frac{\partial}{\partial r}(rv)+\frac{\partial u}{\partial z} = 0, \tag{3}$$

with the boundary conditions

$$u = 0, \quad v = 0 \quad \text{for} \quad z = 0, \quad 0 \leqslant r < 1, \tag{4}$$

$$u = 1-2r^2, \quad v = 0 \quad \text{for} \quad z = \infty, \quad 0 \leqslant r \leqslant 1, \tag{5}$$

$$u = -1, \quad v = 0 \quad \text{for} \quad 0 \leqslant z < \infty, \quad r = 1, \tag{6}$$

$$\partial u/\partial r = 0, \quad v = 0 \quad \text{for} \quad 0 \leqslant z < \infty, \quad r = 0, \tag{7}$$

where (dimensional quantities having an asterisk)

$$u = u^*/\bar{u}, \quad v = v^*/\bar{u} \tag{8}$$

denote the axial and radial velocity components,

$$z = z^*/R, \quad r = r^*/R \tag{9}$$

the axial and radial distance variables,

$$p = p^*/\rho\bar{u}^2 \tag{10}$$

the dimensionless pressure and

$$Re = 2\rho R\bar{u}/\mu \tag{11}$$

the Reynolds number. Here $\bar{u}$ is the velocity of the piston in 'tube space', which is equal to the absolute value of the velocity of the tube walls in 'piston space'. $R$ is the radius of the tube, $\rho$ the density and $\mu$ the viscosity. The origin of the co-ordinate system is assumed to be at the fixed piston head.

Equations (1)–(3) lead to the familiar vorticity transport equation

$$\frac{\partial}{\partial r}\left(\frac{\omega}{r}\frac{\partial\psi}{\partial z}\right) - \frac{\partial}{\partial z}\left(\frac{\omega}{r}\frac{\partial\psi}{\partial r}\right) = \frac{2}{Re}\left[\frac{\partial^2\omega}{\partial z^2} + \frac{\partial}{\partial r}\left(\frac{1}{r}\frac{\partial}{\partial r}(r\omega)\right)\right] \tag{12}$$

on eliminating the pressure gradients and introducing the dimensionless stream function $\psi$ and the dimensionless vorticity $\omega$:

$$u = -\frac{1}{r}\frac{\partial\psi}{\partial r}, \quad v = \frac{1}{r}\frac{\partial\psi}{\partial z}, \quad \omega = \frac{\partial v}{\partial z} - \frac{\partial u}{\partial r}. \tag{13)–(15}$$

It follows from (13)–(15) that the vorticity $\omega$ is related to the stream function $\psi$ by

$$\omega r = \frac{\partial^2\psi}{\partial z^2} + \frac{\partial^2\psi}{\partial r^2} - \frac{1}{r}\frac{\partial\psi}{\partial r}. \tag{16}$$

The two coupled elliptic equations (12) and (16), together with suitable boundary conditions for the stream function $\psi$ and the vorticity $\omega$, give a complete description of the velocity field for the system under consideration.

## 3. Boundary conditions for stream function $\psi$ and vorticity $\omega$

The main difficulty in solving the boundary-value problem for the fourth-order system of differential equations (12) and (16) is the specification of suitable boundary conditions. So far it is unclear for which boundary conditions the problem is well defined. It is assumed here that Dirichlet or Neumann boundary conditions for $\psi$ and $\omega$ over the entire region of the flow field are sufficient to generate unique and stable solutions. The following boundary conditions were used:

$$\psi = 0, \quad \omega = r^{-1}\partial^2\psi/\partial z^2 \quad \text{for} \quad z = 0, \quad 0 \leqslant r < 1, \tag{17}$$

$$\psi = \tfrac{1}{2}(r - r^2), \quad \omega = 4r \quad \text{for} \quad z = \infty, \quad 0 \leqslant r \leqslant 1, \tag{18}$$

$$\psi = 0, \quad \omega = -1 + \partial^2\psi/\partial r^2 \quad \text{for} \quad 0 \leqslant z < \infty, \quad r = 1, \tag{19}$$

$$\psi = \omega = 0 \quad \text{for} \quad 0 \leqslant z < \infty, \quad r = 0. \tag{20}$$

A singularity occurs at the piston–wall junction, where the velocity has the two values of zero (fixed piston head) and the wall speed, because of the idealized abstraction used of motion of a piston in a tube without leakage. Different boundary values at the corner were used for the vorticity, which changes from high positive to low negative values near the corner at low Reynolds numbers (figure 3*a*). At higher Reynolds numbers, this change occurs further inwards on the piston head (figure 3*b*). It was found that the area affected was small and restricted to the immediate vicinity of the corner, and that the best results were obtained by treating the corner as a regular wall point.

Owing to the necessity of using a numerical procedure to solve the system of nonlinear partial differential equations, a co-ordinate transformation has to be applied to map the infinite region $0 \leqslant z \leqslant \infty$ onto a finite region. The following transformation has proved to be useful:

$$\xi = \tanh az. \tag{21}$$

The complete flow field is therefore mapped onto the region $0 \leqslant \xi \leqslant 1$. By a proper choice of the constant $a$, the region near $z = 0$, which is of special importance for this flow, can be stretched deliberately. The differentials $\partial/\partial z$ and $\partial^2/\partial z^2$ have to be replaced everywhere by

$$\partial/\partial z = a(1-\xi^2)\,\partial/\partial\xi \tag{22}$$

and

$$\partial^2/\partial z^2 = a^2(1-\xi^2)^2\,\partial^2/\partial\xi^2 - 2a^2\xi(1-\xi^2)\,\partial/\partial\xi. \tag{23}$$

## 4. Numerical solution by an implicit finite-difference method

A grid with $K$ columns (subscript $k$) and $L$ rows (subscript $l$) was imposed on the flow field. A standard central-difference approximation with a leading error of second order was applied to the space derivatives. The finite-difference equations which result from (12) and (16) can be represented for every interior point $(k, l)$ of the grid by

$$\begin{aligned}\omega_{k,l} = {} & W_{k+1,l+1}\,\omega_{k+1,l+1} + W_{k-1,l+1}\,\omega_{k-1,l+1} \\ & + W_{k+1,l-1}\,\omega_{k+1,l-1} + W_{k-1,l-1}\,\omega_{k-1,l-1}\end{aligned} \tag{24}$$

and

$$\begin{aligned}\psi_{k,l} = {} & P_{k+1,l+1}\,\psi_{k+1,l+1} + P_{k-1,l+1}\,\psi_{k-1,l+1} \\ & + P_{k+1,l-1}\,\psi_{k+1,l+1} + P_{k-1,l-1}\,\psi_{k-1,l-1} \\ & + W_{k,l}\,\omega_{k,l},\end{aligned} \tag{25}$$

where the coefficients $P_{k\pm1,l\pm1}$ and the coefficient $W_{k,l}$ are functions of $r$ and $\xi$ only while the coefficients $W_{k\pm1,l\pm1}$ are functions of $r$, $\xi$ and all the $\psi_{k\pm1,l\pm1}$. All coefficients are explicitly given by Vrentas *et al.* (1966).

An 'extrapolated Liebmann' or 'successive over-relaxation' (SOR) method (Smith 1974, p. 149) was used to solve the system of equations (24) and (25) iteratively for all points of the finite-difference network. For this purpose, initial values were assumed for $\psi$ and $\omega$ throughout the interior of the grid and for $\omega$ on the tube wall and the piston head. By use of (25), new values of $\psi$ were

| | $\psi$ | | |
|---|---|---|---|
| $\xi = 0{\cdot}5$ | 21 × 21 mesh points | 41 × 41 mesh points | 61 × 61 mesh points |
| $r = 0$ | 0 | 0 | 0 |
| 0·1 | −0·003116 | −0·003112 | −0·003110 |
| 0·2 | −0·012320 | −0·012314 | −0·012312 |
| 0·3 | −0·027148 | −0·027144 | −0·027144 |
| 0·4 | −0·046580 | −0·046588 | −0·046590 |
| 0·5 | −0·068640 | −0·068670 | −0·068678 |
| 0·6 | −0·089790 | −0·089850 | −0·089866 |
| 0·7 | −0·104150 | −0·104226 | −0·104246 |
| 0·8 | −0·102704 | −0·102768 | −0·102782 |
| 0·9 | −0·073018 | −0·073036 | −0·073042 |
| 1·0 | 0 | 0 | 0 |
| $r = 0{\cdot}5$ | | | |
| $\xi = 0$ | 0 | 0 | 0 |
| 0·1 | −0·006194 | −0·006170 | −0·006166 |
| 0·2 | −0·020734 | −0·020680 | −0·020672 |
| 0·3 | −0·038152 | −0·038118 | −0·038114 |
| 0·4 | −0·054744 | −0·054750 | −0·054754 |
| 0·5 | −0·068640 | −0·068670 | −0·068678 |
| 0·6 | −0·079238 | −0·079268 | −0·079276 |
| 0·7 | −0·086624 | −0·086634 | −0·086638 |
| 0·8 | −0·091180 | −0·091162 | −0·091160 |
| 0·9 | −0·093388 | −0·093340 | −0·093330 |
| 1·0 | −0·093750 | −0·093750 | −0·093750 |

TABLE 1. Effect of mesh size ($Re = 10$, $a = 1$, $F = 1{\cdot}22$)

calculated and further improved by the SOR method, which is essentially an extrapolation scheme

$$\psi = F\psi_{\text{new}} + (1-F)\,\psi_{\text{old}}; \tag{26}$$

$F$ is the over-relaxation factor. As equations (24) are coupled to (25) by the boundary conditions (17) and (19), which read in finite-difference form

$$\omega_{1,l} = \frac{a^2}{2r(\Delta\xi)^2}(8\psi_{2,l} - \psi_{3,l}) \tag{27}$$

and

$$\omega_{k,L} = -1 + \frac{1}{(2\Delta r)^2}(8\psi_{k,L-1} - \psi_{k,L-2} + 6\Delta r), \tag{28}$$

improved values for $\omega$ could be obtained subsequently at the tube wall and the piston head. The extrapolation scheme described above was now applied to all $\omega$ values at the interior points of the region.

This procedure was iterated and proved stable and convergent for a proper choice of the over-relaxation factor $F$, which was of the order of 1·22. Improved values were used as soon as available. The finite-difference solution was considered to have converged when the $\psi$ and $\omega$ values changed by less than 0·1 % at all grid points from one iteration to the next. Special attention was given to

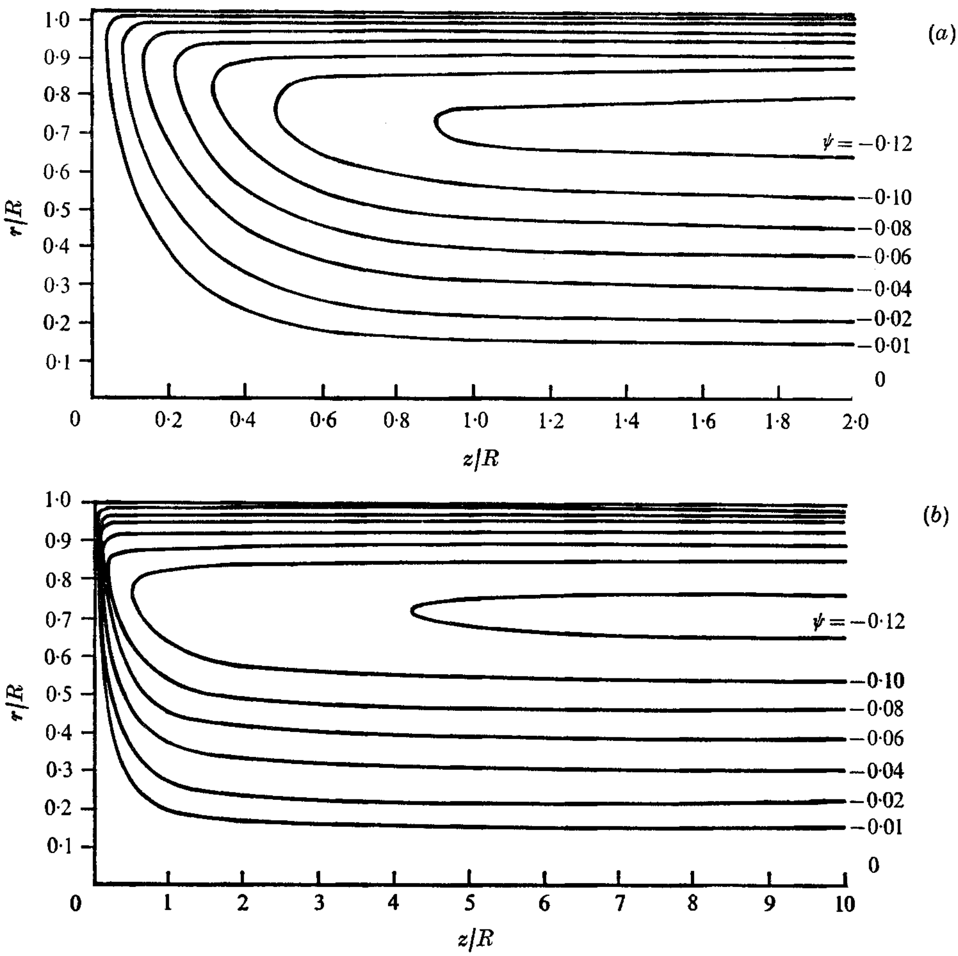


FIGURE 2. Streamlines for (*a*) $Re = 10$ and (*b*) $Re = 400$.

the mesh size necessary to keep the discretization error small. All calculations were performed with a $61 \times 61$ point grid. Some typical effects of increasing the mesh size are shown in table 1. The $\psi$ values at coinciding grid points for a $41 \times 41$ and a $21 \times 21$ grid differ by less than 0·1 % and 1 % respectively from the $\psi$ values for the $61 \times 61$ grid.

## 5. Results and discussion

Calculations were performed for Reynolds numbers from 0 to 800, and the results of the numerical solution of the full Navier–Stokes equations are presented in figures 2–7.

No flow separation was observed at the 90° corner between the piston head and the tube wall, in accordance with the work of Gerrard (1971). Typical distributions of streamlines are given in figures 2 (*a*) and (*b*) for Reynolds numbers of 10 and 400 respectively; the basic streamline pattern remains practically unchanged for all Reynolds numbers considered except for stretching in the

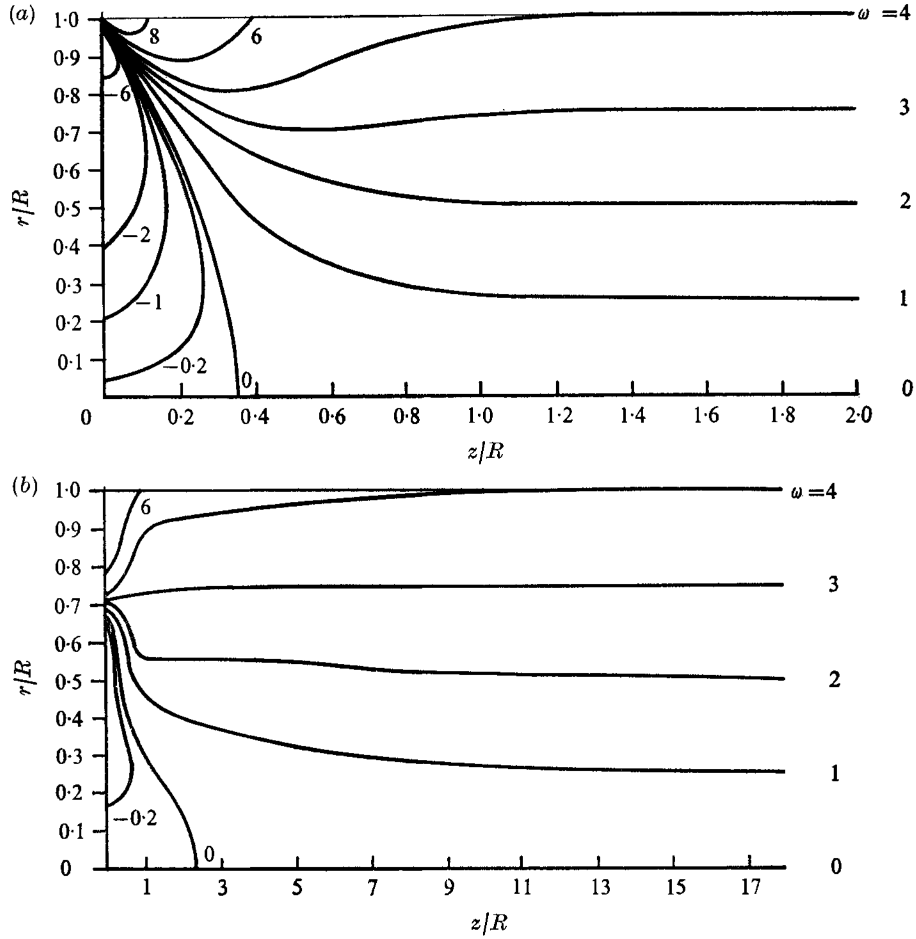


FIGURE 3. Equi-vorticity lines for (a) $Re = 10$ and (b) $Re = 400$.

axial direction. The corresponding vorticity distributions are illustrated in figures 3(a) and (b). At low Reynolds numbers (figure 3a), the diffusive terms in the vorticity transport equation (12) are dominant. At higher Reynolds numbers, distortion of the vorticity distribution is caused by the convective terms (figure 3b).

The velocity distribution was calculated by use of (13) and (14) and retransformed into 'tube space'. Results are given in figures 4 and 5. At low Reynolds numbers, the axial velocity profile remains essentially flat for some distance $z$ in front of the piston head with a slight concavity near the centre of the tube for small $z$ (figure 4a). At higher Reynolds numbers, this concavity becomes much more pronounced and the velocity distribution exhibits two symmetrical maxima separated by a local minimum on the tube axis (figure 4b). Similar behaviour was observed by Friedmann *et al.* (1968) as well as Vrentas & Duda (1973) for their respective entrance-flow models. As Vrentas & Duda (1973) pointed out, this phenomenon occurs in regions where the vorticity is small compared with $\partial v/\partial z$ and $\partial v/\partial z$ is positive. From (15), this obviously leads to the result that $du/\partial r$ must be positive so that the axial velocity does not decrease

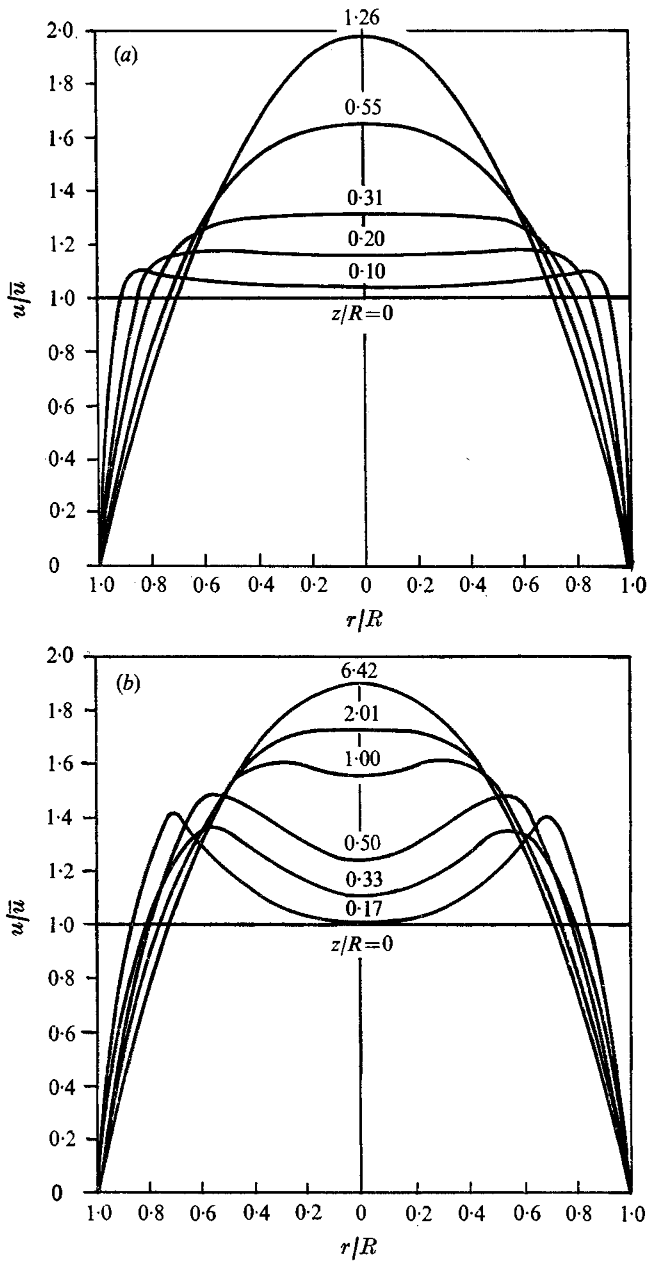


FIGURE 4. Development of axial velocity for (*a*) $Re = 10$ and (*b*) $Re = 400$.

monotonically from its centre-line value. The radial velocity profile for $Re = 10$ is presented in figure 5.

The dimensionless entrance length $Z_E$ is defined in the usual way as the dimensionless axial position, measured from the position of the piston head, at which the axial velocity at the centre-line reaches 99 % of its fully developed value. The entrance length $Z_E$ shows a linear increase with increasing Reynolds number for high $Re$ and a limiting value of $Z_E = 1{\cdot}45$ for $Re = 0$ (figure 6).

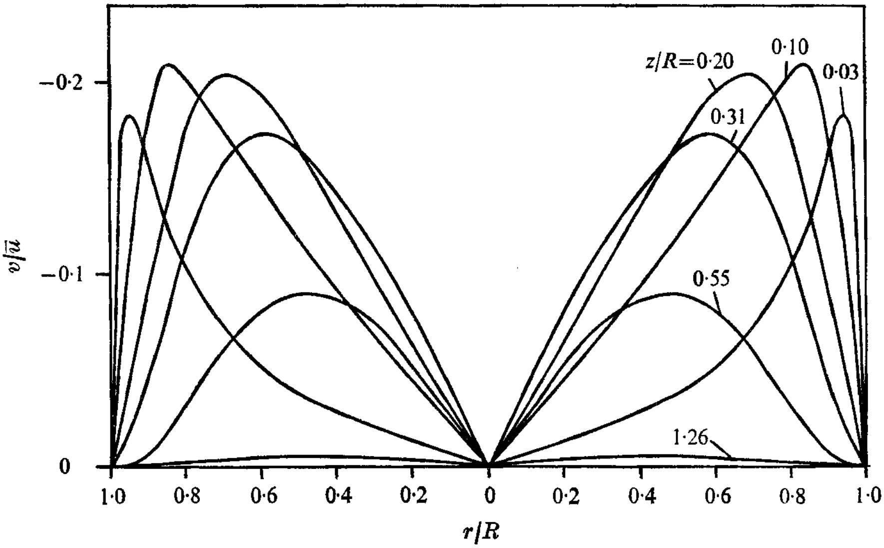


FIGURE 5. Development of radial velocity for $Re = 10$.

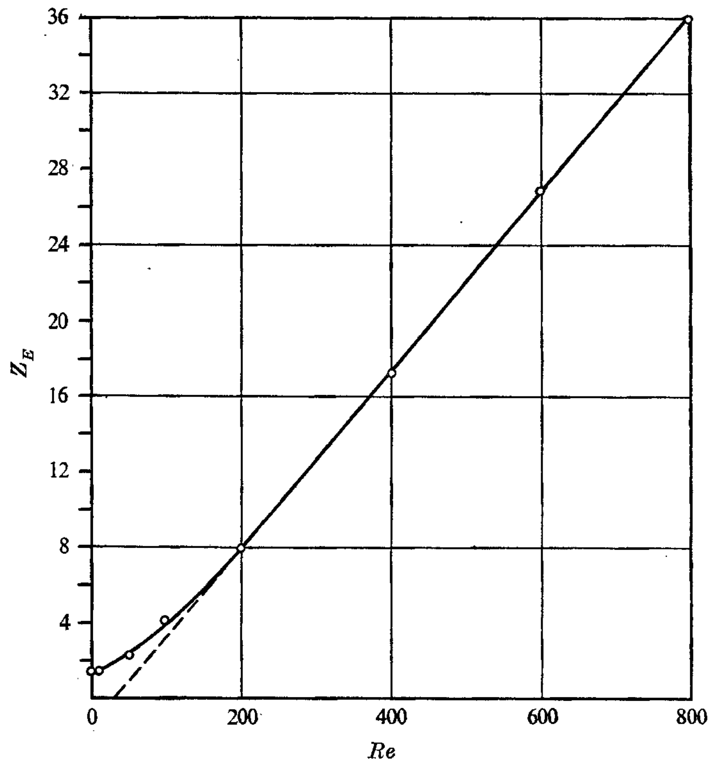


FIGURE 6. Dependence of dimensionless entrance length $Z_E$ on Reynolds number $Re$. ---, $Z_E = 0{\cdot}0475\,Re - 0{\cdot}8$.

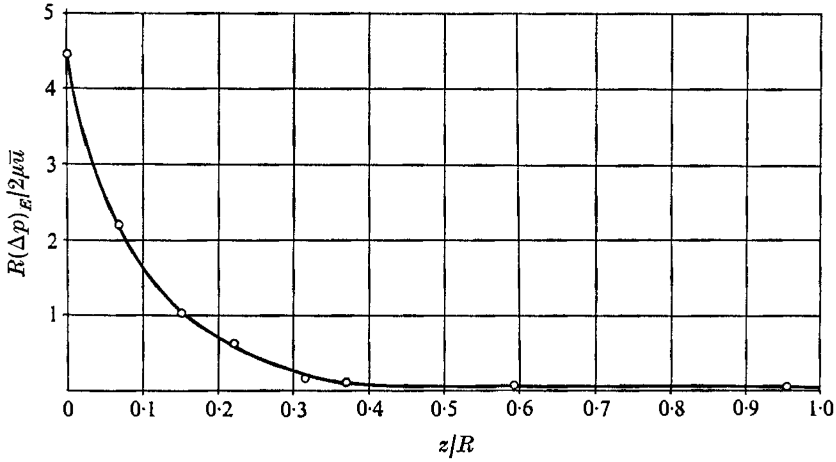


FIGURE 7. Axial decay of excess pressure for $Re = 10^{-6}$.

The excess pressure drop $\Delta p_E$, that is, the total pressure drop in the system minus the pressure drop that would result in fully developed tube flow, is given by

$$\frac{R\Delta p_E}{2\mu\bar{u}} = \frac{Re}{8} + \int_{r=0}^{1}\int_{z=0}^{\infty} (\tfrac{1}{2}I_2 - 16r^2)\, r\, dr\, dz, \tag{29}$$

where $I_2$ is the second invariant of the rate-of-strain tensor:

$$I_2 = 2\left[\left(\frac{\partial v}{\partial r}\right)^2 + \left(\frac{\partial u}{\partial z}\right)^2\right] + \left[\frac{\partial v}{\partial z} + \frac{\partial u}{\partial r}\right]^2. \tag{30}$$

Convergence of the double integral comprising the infinite flow field is secured, as $I_2$ rapidly approaches a value of

$$\lim_{z\to\infty} I_2 = 32r^2. \tag{31}$$

For $Re = 10^{-6}$, when the kinetic-energy term in (29) can be neglected, the axial dependence of

$$\frac{R\Delta p_E(z)}{2\mu\bar{u}} = \int_{r=0}^{1}\int_{z}^{\infty} (\tfrac{1}{2}I_2 - 16r^2)\, r\, dr\, dz, \tag{32}$$

which is due to viscous dissipation only, is shown in figure 7. The double integral is weakly dependent on the Reynolds number, increasing with increasing $Re$.

The dimensionless extra length of tube needed to account for the excess pressure drop is given by

$$Z_p = R\Delta p_E/8\mu\bar{u}. \tag{33}$$

Therefore $Z_p$ is of the order of one tube radius for small $Re$ and approximately equal to $\frac{1}{32}Re$ for high Reynolds numbers.

The author wishes to thank Professor Dr G. Schenkel for valuable discussions and his continuous interest in the progress of this work. Financial support from the Deutsche Forschungsgemeinschaft (DFG) is gratefully acknowledged.

## REFERENCES

FRIEDMANN, M., GILLIS, J. & LIRON, N. 1968 Laminar flow in a pipe at low and moderate Reynolds numbers. *Appl. Sci. Res.* A **19**, 426.

GERRARD, J. H. 1971 The stability of unsteady axisymmetric incompressible pipe flow close to a piston. *J. Fluid Mech.* **50**, 625.

GERRARD, J. H. & HUGHES, M. D. 1971 The flow due to an oscillating piston in a cylindrical tube: a comparison between experiment and a simple entrance flow theory. *J. Fluid Mech.* **50**, 97.

HUGHES, M. D. & GERRARD, J. H. 1971 The stability of unsteady axisymmetric incompressible pipe flow close to a piston. Part 2. Experimental investigation and comparison with computation. *J. Fluid Mech.* **50**, 645.

SCHLICHTING, H. 1934 Laminare Kanaleinlaufstroemung. *Z. angew. Math. Mech.* **14**, 368.

SCHMIDT, F. W. & ZELDIN, B. 1969 Laminar flows in inlet sections of tubes and ducts. *A.I.Ch.E. J.* **15**, 612.

SMITH, G. D. 1974 *Numerical Solution of Partial Differential Equations.* Oxford University Press.

SPARROW, E. M., LIN, S. H. & LUNDGREN, T. S. 1964 Flow development in the hydrodynamic entrance region of tubes and ducts. *Phys. Fluids*, **7**, 338.

TABACZYNSKI, R. J., HOULT, D. P. & KECK, J. C. 1970 High Reynolds number flow in a moving corner. *J. Fluid Mech.* **42**, 249.

VAN DYKE, M. 1970 Entry flow in a channel. *J. Fluid Mech.* **44**, 813.

VRENTAS, J. S. & DUDA, J. L. 1973 Flow of a Newtonian fluid through a sudden contraction. *Appl. Sci. Res.* **28**, 241.

VRENTAS, J. S., DUDA, J. L. & BARGERON, K. G. 1966 Effect of axial diffusion of vorticity on flow development in circular conduits. Part I. Numerical solutions. *A.I.Ch.E. J.* **12**, 837.

WILSON, S. D. R. 1971 Entry flow in a channel. Part 2. *J. Fluid Mech.* **46**, 787.